

MANUFACTURABILITY ANALYSIS OF CRUMPLE-FORMED GEOMETRIES THROUGH REDUCED ORDER MODELS

Olivia Trautschold* and Andy Dong*

*School of Mechanical, Industrial, and Manufacturing Engineering,
Oregon State University, Corvallis, OR 97331

Abstract

Crumple-formed structures have irregular, multiscale geometric complexity. Similar to periodic lattices, crumpled geometries can be tailored to applications requiring a high strength-to-weight ratio. As an alternative to confinement-based crumple forming, additive manufacturing allows for increased geometric control and structural reproducibility to fabricate these structures. The inherently irregular geometries of crumple-formed structures decrease the sensitivity of macroscale properties to microscale manufacturing defects but pose a unique challenge for the analysis of manufacturability using additive processes. Current approaches to manufacturability analysis lack techniques suitable for addressing the multiscale geometric complexity and irregularity of crumpled structures. This paper presents a preliminary study into the manufacturability of crumple-formed structures using a model reduction technique that preserves the robust bulk statistical properties of crumpled structures. Manufacturability predicted by the reduced order model is assessed against an ideal geometry for additive processes.

Keywords: crumple-forming, additive manufacturing, manufacturability analysis, complex network theory, eigenvalue decomposition

Introduction

Layer-by-layer additive manufacturing (AM) processes allow designers to explore increasingly complex and irregular geometries for which manufacturing would be impractical with subtractive or forming methods. There is continued interest in developing rapid manufacturability analysis tools to provide new and experienced designers with preliminary information about feasible geometries for AM [1]. Integrating manufacturability analysis tools into the early design process will allow designers to iterate through novel geometries prior to physical prototyping. A concurrent approach to design and analysis also provides designers with initial understanding of the potential for structural deviation between an intended design and the manufactured outcome.

This study explores methods to analyze the manufacturability of complex, irregular, crumple-formed structures by additive processes. Crumpled geometries are prevalent in nature, from the cortical surface of a mammalian brain [2] to faults along tectonic plate boundaries [3]. Recent studies into controlled crumpling include nanoscale graphene-based composites for supercapacitor applications [4], lightweight, energy absorbing materials for automobile crumple zones [5], and crumple-formed metamaterials for improved biological tissue regeneration [6]. Fundamental research into the dynamics of crumpling reveal the presence of irregular yet hierarchical architectures with customizable properties such as porosity, stiffness, and surface functionalization [7]. While existing publications explore the physical phenomena of crumpling

and diverse applications for crumpled geometries, this paper presents a novel investigation into the manufacturability of crumpled structures through additive processes.

As an alternative to deformation-based crumpling of thin sheets of material, layer-by-layer AM has the potential to provide designers with increased control over crumpled geometries on multiple length scales. This elevated control may subsequently enable designers to tailor the physical and mechanical properties of crumpled structures. AM also enables the manufacture of replicates from simulated, computer-aided design (CAD) models, whereas real deformation-based crumpling will always result in a unique internal structure. In turn, AM may provide more reproducible and controlled bulk statistical properties than are attainable by deformation-based fabrication. However, before AM can be considered a viable alternative for crumpled structure fabrication, a suitable manufacturability analysis method must be developed. The multiscale complexity and irregular features of crumpled thin sheets pose a challenge for existing manufacturability analysis methods. The disordered ridge network in crumpled geometries produce an inhomogeneous distribution of voids and overhang regions, and the complex internal topology and fine features will not be amenable to the generation or removal of internal support structures.

The proposed approach to manufacturability evaluation is based in network theory, specifically the topological analysis of complex networks. In this preliminary implementation, a reduced-order model of crumpled geometry is achieved by approximating the simulated crumple-formed structure as a network representation. The network representation is produced by a low-dimensional model of the crumple-form structure through eigenvalue decomposition (EVD). The low-dimensional model eliminates noise produced by randomly distributed geometric features to find a set of modes that represent coherent structures in the crumpled form. These coherent structures, represented as connected networks, enable manufacturability analysis. Due to the exploratory scope of this research, the proposed manufacturability analysis model is currently limited to theoretical validation against a simple geometry suitable for additive processes. A case study is performed to compare the manufacturability of the ideal geometry against crumpled structures with varying degrees of compaction.

Background

Crumpled structures are presently fabricated by deformation of a thin sheet of material within a boundary region. Crumpling occurs as the confined thin sheet exhibits a material-dependent elasto-plastic response that localizes deformation along ridges and vertices [8]. In the context of crumpled geometries, microstructure is composed of discrete ridges and vertices. Mesostructure arises in the form of a network of ridges and vertices across the thin sheet, and the crumpled macrostructure is represented by the external form of the crumpled geometry. Macrostructure often approximates the shape of the boundary region, particularly at high compaction ratios (Figure 1). Macrostructure is also represented in the bulk statistical properties of the crumpled geometry. When a thin sheet of material is crumpled, its macrostructure transforms from a flat, thin sheet to a low-density three-dimensional structure with improved impact absorption capabilities [8]. Despite an inherently disordered distribution of ridges and vertices, approximating the bulk statistical properties of crumpled geometries has been demonstrated to correlate to macroscale properties [9]. Also, unlike periodic lattice or origami structures which are

highly sensitive to mesoscale manufacturing imperfections, crumple-formed geometries demonstrate reduced sensitivity to microscale and mesoscale structural defects [6], [8]. This unique, robust characteristic of crumpled geometries minimizes the impact of small-scale manufacturing defects on macroscale properties. Moreover, the robust macrostructure may exhibit less sensitivity to the part-to-part variability shown in many AM fabrication processes.

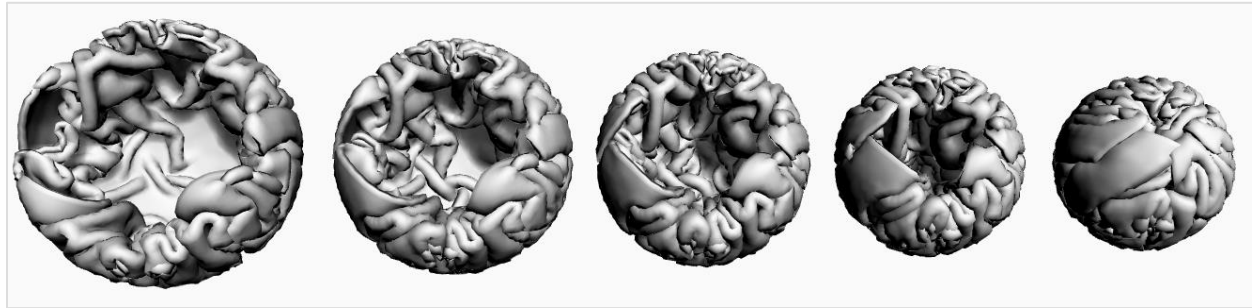


Figure 1 Crumpled thin sheet formed by simulated spherical confinement, compaction increasing from 20% to 100% in 20% increments (left to right).

While AM methods are capable of producing delicate geometries and complex internal features that are not feasible for subtractive or forming manufacturing methods, each AM process imposes a unique set of design constraints. A common topological constraint in many AM methods are overhangs, or material deposited over a void space that is not sufficiently supported from below [10]. Overhang regions may sag or break during fabrication, resulting in defects in the structure. Other AM constraints include dimensional parameters such as minimum feature size and maximum build volume [11], which respectively constrain the microscale and macroscale geometry. Continued interest in manufacturability analysis techniques is driven by the incorporation of AM knowledge and constraints into the early design process to reduce downstream design changes.

Existing approaches to manufacturability analysis vary depending on the structure, metrics, and AM process of interest. One existing approach to evaluate the manufacturability of complex, multiscale geometries is through model reduction by homogenization using a representative volume element or unit cell. This approach is suitable for the periodic complexity found in ordered lattice structures [12]. However, crumpled geometries do not possess a uniform, representative volume element necessary for model reduction by homogenization. Other approaches range from case-by-case design heuristics [11] to neural networks for topological feature recognition [13]. It is not feasible to rely on a set of crisp heuristics to evaluate crumpled geometries due to the inherent disorder and hierarchical geometric complexity in these structures. The computational cost of applying design rules on multiple length scales becomes intractably expensive to model, and the inter-scale effects of topological changes can be difficult to predict.

Emergent techniques for the reduction of structures with multi-dimensional complexity into low-dimensional models have applications ranging from materials design to systems design. On the materials level, Li et al. developed a dimensionality reduction technique to lower the computational expense of modeling polycrystalline microstructures while retaining their statistical properties [14]. In the realm of Design for Additive Manufacturing (DfAM), Coatanéa et al. developed a low-dimensional model to rank part geometries and their performance based on multiple manufacturability metrics [15]. Like the case study presented in this paper, Coatanéa et

al. demonstrate their manufacturability analysis method by evaluating multiple alternative geometries against an ideal form. However, the analysis approach by Coatanéa et al. is more prescriptive than predictive, as their model requires prior evaluation of individual parts' performance based on each manufacturability metric. Due to the hierarchical complexity and limited experimental data on additively manufactured crumple-formed geometries, model reduction in this paper is performed directly on a network representation of the part geometry rather than reducing a matrix of multiple geometries with pre-determined manufacturability metrics. Integration of network theory and model reduction has been previously demonstrated by Dong et al., in which network theory and singular value decomposition (SVD) were implemented to model the complexity of a knowledge structure associated with emergent technology [16]. The network topology properties were then evaluated to forecast the product innovation potential. Sarkar et al. also employed network theory and eigenvalue decomposition (EVD) to analyze the modularity of complex product architectures in terms of their implications for system resilience [17]. These studies have developed an understanding how eigenvectors behave under variations in the underlying structure. Coherent structures calculated from the eigenmodes serve as the basis for predicting microscale structures up to the macroscale, and their associated functions. This research extends those insights to determine whether coherent network structures can be leveraged to propose generative approaches to form irregular geometries with multiscale complexity.

Research Aim and Hypotheses

In the proposed manufacturability analysis approach based in complex network theory, crumpled geometries are approximated as network representations based upon a low-order network approximations through eigenvalue decomposition. Topological properties of the reduced-order networks are evaluated in terms of geometric complexity of the crumpled structure. The implications of geometric complexity for predicting structural defects during AM processes are also examined. This exploratory study aims to address the following research questions:

1. What does network topology reveal about the crumple-formed mesostructure and the likelihood of structural deviation between the designed and additively manufactured geometry?
2. How does model reduction impact network topology and the subsequent manufacturability evaluation?

To address these research questions within the scope of this preliminary study, a case study is performed to evaluate the mesostructure complexity of crumpled geometries at varying compaction ratios in relation to a solid sphere. Crumpled structures evaluated in this study approximate a spherical macrostructure (Figure 1), so a solid sphere is selected to highlight geometric variation on sub-macro length scales. A solid sphere manufactured from homogeneous material does not contain any complex or irregular internal features that may give rise to manufacturing defects, whereas thin sheets crumple-formed by spherical confinement contain complex, inhomogeneous internal topology. Mesostructure complexity in crumpled geometries may include thin features, intersecting faces, and internal overhangs. In response to the first research question, it is hypothesized that manufacturability increases as the mesoscale network topology approximates that of a solid sphere.

In response to the second research question, it is hypothesized that the reduced-order network representation reveals underlying geometric complexity in the crumpled structure that is obscured by noise in the high-order network approximation. By examining the eigenvalue spectrum obtained from the network adjacency matrix and reducing the network representation to its significant eigenvalues, the resulting network no longer contains spatial ‘noise’ represented by insignificant eigenvalues. Therefore, by removing redundant or insignificant geometric information from the network approximation, underlying coherent structures may become more apparent. In turn, the reduced-order network may provide a more sensitive depiction of complexity present in the crumpled geometry.

Methodology

This section details the proposed procedure for describing complex, crumple-formed hierarchical geometries through reduced-order network models for manufacturability analysis. The methodology for this research was developed to address the hypotheses put forth in the previous section and restated as follows:

- i. ‘Manufacturability increases as the mesoscale network topology approximates that of a solid sphere.’
- ii. ‘The reduced-order network representation reveals underlying geometric complexity in the crumpled structure.’

The methodology starts with the computational simulation of a crumple-formed mesh geometry. The specific CAD software and physics simulation process are not integral to the network approximation, so the crumpling method employed in this paper is briefly described herein. The crumpled geometries are generated in Rhinoceros 3D CAD software using the integrated Grasshopper visual programming language and Kangaroo live physics engine. Kangaroo is a Grasshopper plugin used to simulate the dynamic spherical confinement of a thin sheet. This is achieved by shrinking a spherical shell around a two-dimensional triangular mesh ‘sheet’. Self-avoidant collision spheres are centered at each vertex in the triangular mesh during crumpling to reduce self-intersection as the mesh is deformed. The self-avoidant sphere diameter is equal to the distance between vertices (0.25 mm) and serves as the thickness dimension for the planar mesh. Similar approaches to simulated crumpling by spherical confinement of a triangular mesh have been employed by Tallinen et al. [18], and Vliegenthart et al. [19]. The case study analyzed in this report investigates the effects of varying the compaction ratio of the crumpled geometry. The self-avoidant spheres centered at each vertex provide thickness to the mesh sheet, so the compaction ratio is the total volume of self-avoidant spheres in the mesh to the final confinement sphere volume. The fully dense sphere is approximated for the case study by generating a spherical confinement mesh and filling it with tightly packed self-avoidant spheres.

To generate the initial network approximation, coordinate positions at each vertex in the triangular mesh are extracted from the crumpled geometry to generate network nodes. In the network approximation of a solid sphere, nodes are generated based on the centroid positions of each self-avoidant sphere in the structure. A list of edges is generated by measuring the radial distance between each node and connecting nodes within a specified radius (in this case, 0.3 mm because this length includes the 0.25 mm sheet thickness and nodes from adjacent layers). This

dimension may be modified based on the minimum feature size capabilities of the 3D-printer and material of interest. This method of spatial edge generation is employed rather than extracting edges directly from the CAD model, because triangular mesh edges in the crumpled geometry are identical to the node connections in the flat mesh sheet prior to spherical confinement. Therefore, the triangular mesh edges alone do not provide sufficient information to approximate the crumpled geometry. This limitation is resolved in the spatial, radial distance approach to edge generation because it simultaneously connects nodes along the triangular mesh sheet and across narrow voids or ridges in the structure, providing additional information about the crumpled mesoscale geometry.

The collection of nodes and edges in the crumpled geometry may be plotted as a network graph using the NetworkX Python library [20]. NetworkX is a software package developed for the creation, manipulation, and study of complex networks. Table 1 displays network graphs drawn in NetworkX for each structure analyzed in the case study. An adjacency matrix, \mathbf{A} is generated from the network representation. The number of rows and columns in the $(n \times n)$ adjacency matrix represent each node in the crumpled geometry, where n is the number of nodes in the network. In the unweighted adjacency matrix, $A_{ij} = 1$ if there is an edge connecting the node pair, or $A_{ij} = 0$ if the pair is not connected. \mathbf{A} is a symmetrical matrix because the edge connections are undirected.

The adjacency matrix, \mathbf{A} is decomposed by EVD into the form $\mathbf{A} = \mathbf{V}\mathbf{D}\mathbf{V}^T$, where \mathbf{A} is the $(n \times n)$ adjacency matrix, \mathbf{V} is the $(n \times n)$ orthonormal eigenvector matrix of \mathbf{A} , and \mathbf{D} is the $(n \times n)$ diagonal eigenvector matrix of \mathbf{A} . As demonstrated in reference [17], each edge in the network approximation is expressed as a vector in space, a linear combination of the eigenvector v_i and corresponding eigenvalue λ_i

$$\mathbf{a}_i = [v_{i1}\lambda_0, v_{i2}\lambda_1, \dots, v_{in}\lambda_{n-1}] \quad (1)$$

Dong et al. and Sarkar et al. have previously shown that eigenvalue decomposition, or singular value decomposition for non-square adjacency matrices, are useful for the detection of hierarchical modularity in complex network representations [16], [17], [21]. Plotting eigenvalues or singular values in order of descending magnitude reveals characteristics about the modularity of the spatial network representation (Figure 2 in the case study). The goal of dimensionality reduction is to eliminate spatial noise in the form of low-magnitude eigenvalues, while preserving significant geometric information about the crumpled structure by retaining the k largest eigenvalues and eigenvectors. The k -reduced approximation is then

$$\mathbf{a}_i^{(k)} = [v_{i1}\lambda_0, v_{i2}\lambda_1, \dots, v_{ik}\lambda_{k-1}] \quad (2)$$

The number of eigenvalues retained in the reduced-order representation may be determined by selecting the largest magnitude eigenvalues before the characteristic ‘elbow’ in the eigenvalue spectra. After the elbow, the magnitude change between eigenvalues decays more gradually. Removing low-magnitude eigenvalues has the effect of removing redundant spatial information from the network approximation. Subsequent research will investigate the balance between removing redundant spatial information and minimizing information loss about fine features in the crumpled mesh. By eliminating spatial redundancy, the network is described with fewer edges and

the reduced-order network approximation may reveal geometric complexity that was previously obscured by noise or redundancy in the high-order approximation.

Three topological network properties are evaluated to identify geometric complexity in the network approximations. The first is the size of the giant component. The size of the giant component is evaluated across multiple layers, sliced along one axis in the network. This metric provides an indication of how the deposited layers of material will vary in a layer-by-layer AM process. In the solid sphere, each layer is a fully connected component, so the layer-by-layer variation of the giant component will closely approximate an inverted U-shape when plotted with respect to depth in the structure. In crumpled geometries, the size of the giant connected component will vary depending on the distribution of material in each layer. An ideal, in this case inverted U-shape, distribution of the giant component through the depth of the structure indicates fewer voids or internal overhangs that may give rise to mesostructure manufacturing defects. To compare the crumpled structures to a solid sphere, the geometric ratio of the area under the curve (plotted as giant component size versus depth in the structure, Figure 3) is calculated for the crumpled geometries versus that of a solid sphere. An area ratio approaching 1 indicates that the structure may be suitable for manufacture, while ratios much less than 1 predict that the overall structure may be difficult to manufacture.

The second topological property analyzed in the network approximations is the average shortest path length (ASPL), l , Equation 3. ASPL is the average distance $d(i, j)$ measured as the number of edges along the shortest path between each node pair, over the total nodes n in the network [22].

$$l = \frac{1}{n(n-1)} \sum_{i \neq j} d(i, j) \quad (3)$$


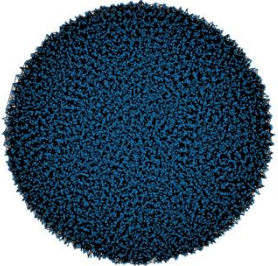
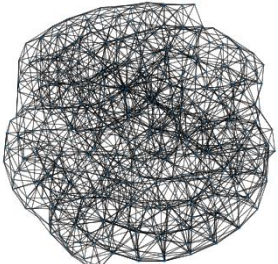
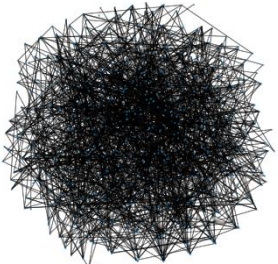
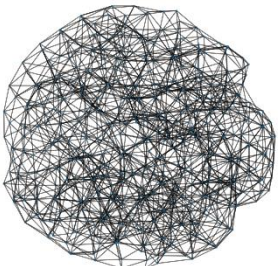
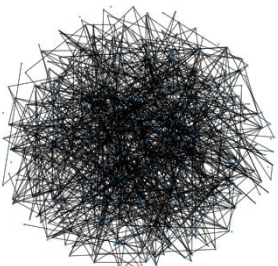
The network representation becomes disconnected after k -reduction. In a disconnected graph ASPL is infinite, and so after model reduction the ASPL is measured for the giant component rather than the entire network. ASPL is an indication of spatial connectivity in the crumpled geometry. Shorter ASPL may relate to a more homogeneous distribution of ridges and fracture surfaces in the crumpled sheet. In terms of manufacturability, shorter ASPL may lead to a more uniform distribution of material across the crumpled mesostructure. More uniform mesoscale material distribution may in turn minimize the risk of structural manufacturing defects propagating across the mesostructure and altering the as-designed macroscale geometry.

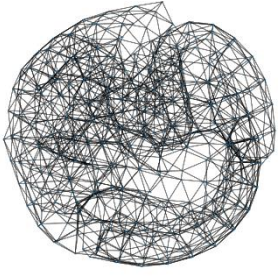
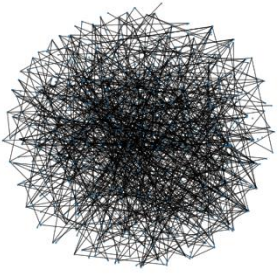
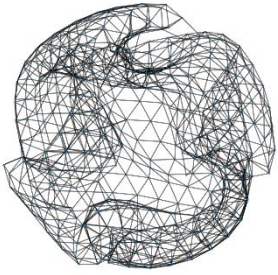
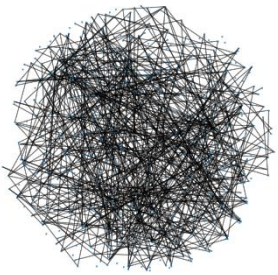
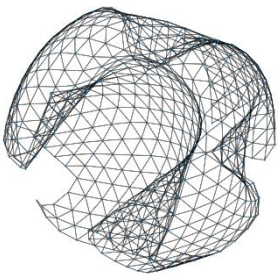

The third and final topological property analyzed in the network approximation is node degree centrality. In an undirected network, node degree centrality is calculated as the number of edges connected to a node. Edges in the high-order network approximations are generated based on radial proximity between nodes, so node degree distribution will provide a preliminary indication of the distribution of material density in the structure. In a homogeneous network, most of the node degrees cluster around the mean [22]. High node degree indicates a dense collection of nodes. In the reduced-order representations, high node degree may indicate a particularly significant region of the crumpled geometry. In terms of manufacturability, a structural defect in this region may have a significant impact on the surrounding mesostructure. It is therefore preferred for the structure to have a homogenous distribution of node degree.

Case Study

The proposed network approximation and model reduction methodology is implemented in a case study investigating the relationship between varied compaction ratio and manufacturability. The crumpled geometries' mesostructure is also evaluated in relation to a solid sphere. A solid sphere is selected as an ideal geometry for AM because it has a homogeneous mesostructure with no internal voids, fine features, or complex topology. Five crumpled structures are generated with identical mesh parameters, varying only the final radius of the confinement sphere to achieve 20%, 40%, 60%, 80%, and 100% compaction. Simulated sheet thickness is 0.25 mm. Graphs of the high-order network approximations for the solid sphere and crumpled geometries are displayed in Table 1. In the high-order network approximation edges are generated by spatial proximity by connecting nodes that are less than or equal to 0.3 mm apart.

Table 1 Network approximations of solid sphere and crumpled thin sheets with varying compaction ratio. Nodes represented by blue dots, edges represented by black lines. Geometries are not shown to scale.

Label	High-Order Model		Reduced-Order Model	
	Network Approximation	Edges	Network Approximation	Edges
Solid Sphere		86713		48308
100% Compaction		3238		1711
80% Compaction		2911		1412

60% Compaction		2653		1252
40% Compaction		2410		1084
20% Compaction		2220		904

To compute reduced order network approximations (also shown in Table 1), an adjacency matrix is generated for each of the high-order network approximations. Eigenvalue decomposition is performed on each of the unweighted, undirected adjacency matrices. The eigenvalue spectra are plotted in Figure 2. A perfectly modular network would exhibit a single, discrete discontinuity between non-zero singular values and singular values with zero magnitude [17]. However, the eigenvalue spectra in Figure 2 reveal a relatively smooth decay for the solid sphere, down to an elbow that encompasses the first 20-25% of eigenvalues in the sphere representation. Hierarchical modularity is evident in eigenvalue spectra as distinct gaps between clusters of eigenvalues of the same magnitude. Hierarchical modularity is most noticeable in the eigenvalue spectra of the crumpled geometry with 60% compaction, and to a lesser extent it also visible as shorter ‘steps’ in the crumpled geometries with 80% and 100% with compaction. The crumpled geometry with 40% compaction does not show eigenvalue hierarchy, but the modularity is shown by distinct gaps between the first 7 eigenvalues. Finally, the crumpled geometry with 20% compaction does not reveal any significant modularity; instead, the eigenvalues gradually decay to an elbow at 30% and then trail off more gradually afterward. In this case study, a conservative reduction is performed by retaining the first 25% of eigenvalues and eigenvectors in the model. Subsequent investigation into the effect of varying the degree of eigenvalue reduction will be performed in follow on research to examine the extent to which the network representation may be reduced without sacrificing significant information about the geometric complexity.

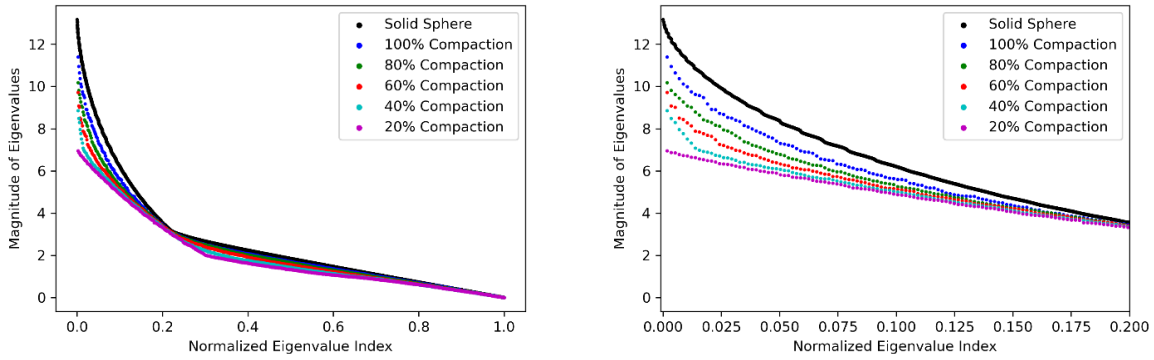


Figure 2 Overlay of eigenvalue spectra full scale (left), and detail (right).

The reduced order network representations are shown in Table 1. After reducing each network to the first 25% of eigenvalues and eigenvectors, the low-dimensional networks no longer retain the same edge connections shown in the high-order approximations. Instead, the redundant spatial information has been eliminated. The reduced networks in Table 1 are plotted with the nodes in their original coordinate positions to visualize the outcome of model reduction; however, the edge lengths and node positions will not impact the subsequent network topology calculations. To demonstrate the effect of visualizing the same network with different node positions, the reduced order model of the crumpled geometry at 80% compaction is plotted in Figure 3. First the network is plotted with the original coordinate node positions, and then with a spring layout that is commonly used in NetworkX.

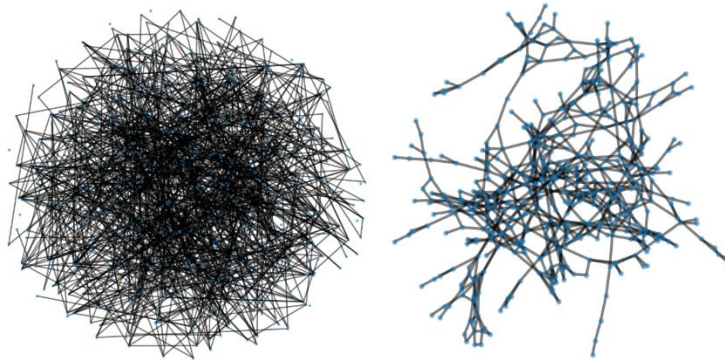


Figure 3 Alternative node positions of the same reduced-order network approximation of the crumpled geometry with 80% compaction.

The first topological network property measured in this case study is variation in the size of the giant component with respect to depth in the structure. For this measurement, the network approximations are segmented based on the coordinate positions of each node. Network nodes are binned by their z-coordinate position to generate subgraphs approximating AM layers of deposited material. Each layer in this case study is 0.25 mm thick, equivalent to the thickness of the simulated, crumpled thin sheet. Giant component size is measured as the largest number of connected nodes across each layer in the structure. Figure 4 displays the giant component size distribution across an ideal homogeneous mesostructure for AM, estimating a solid sphere. The distribution of giant components along the solid sphere approximates an inverted U-distribution because the nodes are densely packed, resulting in a fully connected component across each slice in the structure. Figure 5 displays the giant component size distribution across each layer in the

five crumpled geometries listed in Table 1, before and after dimensionality reduction. In crumpled geometries with 60%, 80%, and 100% compaction, the giant component distributions begin to approximate the inverted U-distribution of the solid sphere in Figure 4. This trend indicates that crumpled geometries at higher compaction ratios more closely approximate the homogeneous mesostructure of a solid sphere. However, after dimensionality reduction through EVD eliminates spatial redundancy in the crumpled geometries, only the geometry at 100% compaction approaches an inverted U-distribution. This discrepancy before and after model reduction in Figure 5 indicates that the reduced-order network approximation may reveal significant geometric complexity by eliminating spatial redundancy in the network.

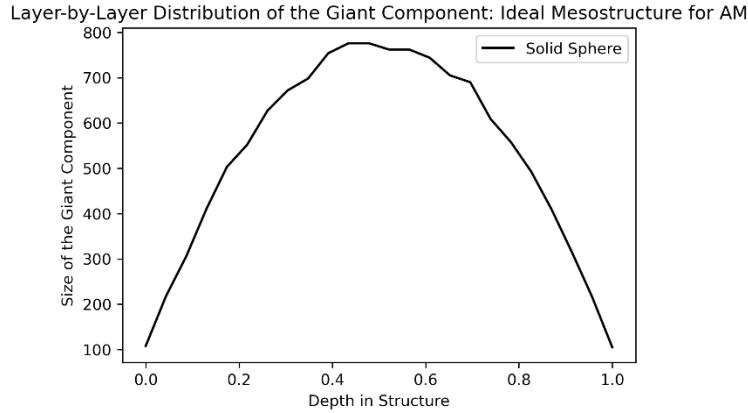


Figure 4 Variation in the size of the giant component across the high-order network approximation of a solid sphere.

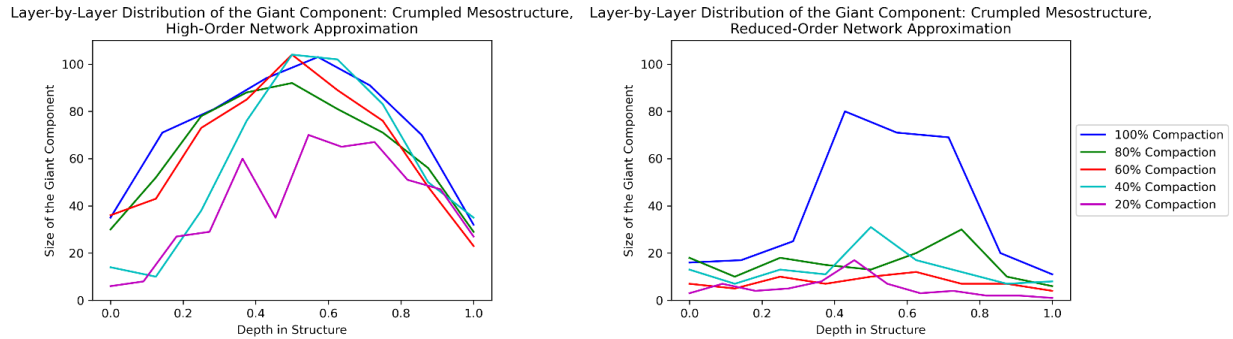


Figure 5 Variation in the size of the giant component across each crumpled network approximation, before and after model reduction.

Figure 6 displays ratios for the area under the curves in Figure 5, comparing the giant component sizes across each crumpled geometry to that of a solid sphere (Figure 4). An area ratio of 1 indicates that the crumpled mesostructure exactly approximates the mesostructure of a homogeneous, solid sphere. The giant component area ratios are monotonically increasing with respect to compaction of the crumpled sheets, both before and after model reduction. Based on this topological network property, crumpled geometry at 100% compaction most closely approximates an ideal mesostructure for AM. This may be due to the dense network of nodes at elevated compaction ratios, approaching homogeneous distribution by reducing void space in the crumpled structure. Comparison of the high-order and reduced-order network approximation in Figure 6 reveals a wider gap in the giant component area ratio between geometries at 80% and 100% compaction in the reduced-order approximation. Therefore, prior to dimensionality reduction this network property may provide an overly optimistic evaluation of the manufacturability of

crumpled geometries at less than 100% compaction. This is attributed to redundant edges in the high-order network approximation obscuring nonhomogeneous geometric features, and artificially increasing the size of the giant component in each layer whereas dimensionality reduction effectively decreases spatial redundancy and reveals underlying geometric complexity in the crumpled geometries.

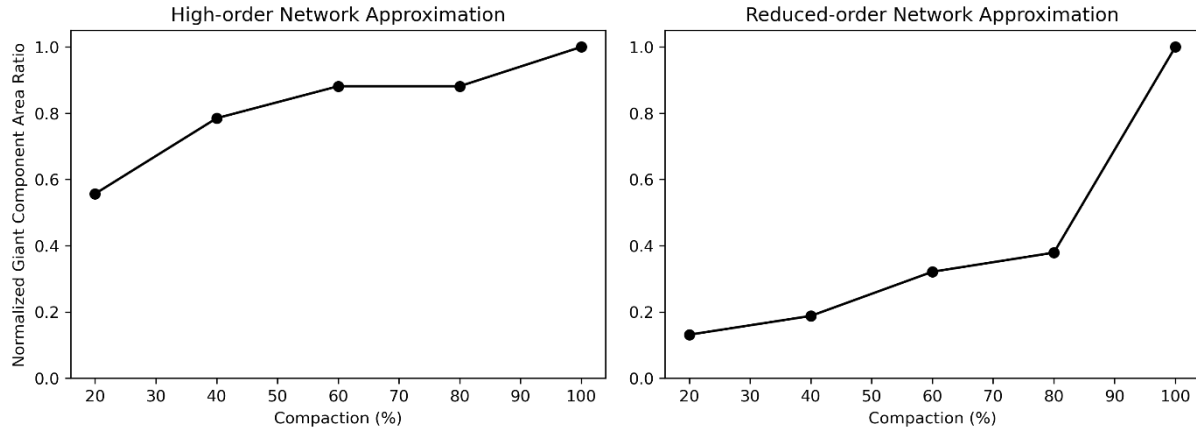


Figure 6 Area ratio under the curves plotted in Figure 5, ratio of the distribution of giant component sizes in each crumpled structure against that of the solid sphere. Results compared for each crumpled geometry before and after model reduction.

The second topological network property analyzed in the case study is the average shortest path length (ASPL). ASPL reveals the average number of network edge connections that span from any node position to any other node in the crumpled geometry. In the event of a disconnected network, ASPL is calculated for the giant component accounting for the full span of z-coordinate positions, rather than the layer-by-layer sub-networks analyzed in the previous metric. In Figure 7, every structure aside from the crumpled geometry at 20% compaction exhibits a longer ASPL after model reduction. This occurs because eliminating redundant spatial information in the network may remove edges that are found along the shortest path between nodes in the structure. In this case, the ASPL relationship to compaction ratio does not follow the same trend before and after model reduction. Prior to model reduction, ASPL is monotonically decreasing with increasing compaction of the crumpled geometry, so the crumpled geometry at 20% compaction has the longest ASPL. However, after model reduction the crumpled structure at 60% compaction has the longest ASPL. The increase in ASPL at 60% compaction in the reduced-order data, is further indication that removing redundant edges and spatial noise reveals underlying complexity in the crumpled geometries. Additionally, maximum ASPL at 60% compaction implies discontinuity in the crumpled mesostructure at intermediate compaction ratios. The results indicate that the crumpled ridge network undergoes a transition phase of an inhomogeneous distribution of ridge lengths between 40% and 80% compaction. A shift in ridge length distribution may occur as the mesostructure transitions from a more homogeneous distribution of long ridges at low compaction (< 40%), to a more homogeneous distribution of short ridges at high compaction (> 80%). ASPL of the ‘ideal’ mesostructure, a solid sphere, is also plotted in Figure 7. ASPL of the solid sphere before and after model reduction is displayed as a straight line in Figure 7 to facilitate visual comparison against the ASPL of the crumpled geometry at each compaction ratio. The results in Figure 7 conflict with the proposed hypothesis that manufacturability increases as the mesoscale network topology approximates that of a solid sphere, because the ASPL of the solid sphere is longer than the ASPL of the crumpled geometries. Instead of relating the crumpled geometries’

ASPL to that of an ideal geometry, it may be sufficient to pursue a minimum ASPL for this manufacturability metric.

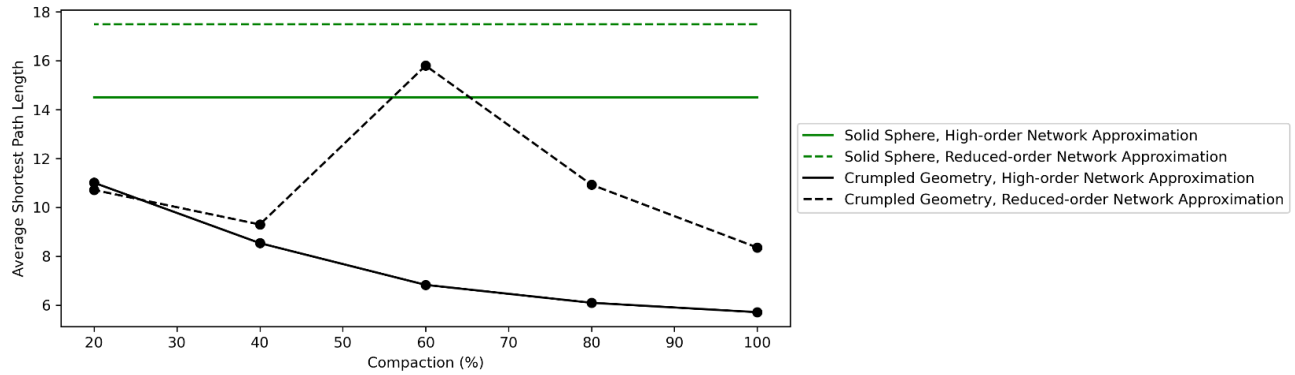


Figure 7 The average shortest path length between each node pair, before and after model reduction.

The final topological network property measured in this case study is node degree centrality, measured as the frequency distribution of the number of edges per node in the network. In the high-order network approximation, high node degree occurs along narrow ridges and tightly folded layers in the crumpled sheet. In the solid sphere, higher node degree is expected at the center of the homogeneous structure, with lower node degree near the perimeter of the solid sphere. Performing model reduction on the network representation of the solid sphere (Figure 8) reveals a more normal frequency distribution of node degrees by eliminating noise in the high-order network. In Figure 9, the crumpled geometries also shift to a more normal distribution of node degrees in the reduced-order network approximations. Comparing the reduced-order node degree distribution in Figure 8 and Figure 9, crumpled geometry at 80% compaction most closely approximates the node degree distribution of the solid sphere. Geometries at 60% and 100% compaction also approach a more normal node degree distribution than is achieved at 20% or 40% compaction.

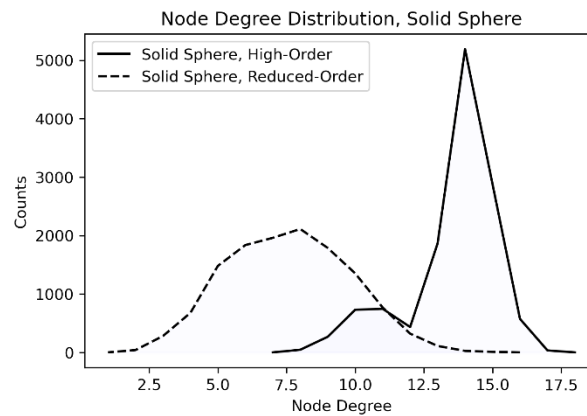


Figure 8 Node degree distribution, solid sphere before and after model reduction.

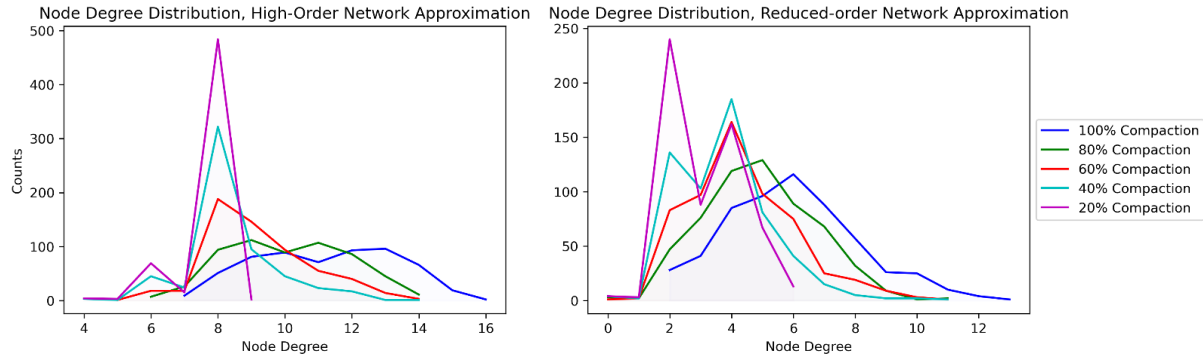


Figure 9 Node degree distribution, crumpled geometries before and after model reduction.

Conclusions

This study serves as a preliminary exploration into the application of complex network theory in conjunction with eigenvalue decomposition for the manufacturability analysis of irregular, crumple-formed geometries with hierarchical complexity. The research questions examine: (1) ‘What does network topology reveal about the crumple-formed mesostructure and the likelihood of structural deviation between the designed and additively manufactured geometry?’; and, (2) ‘How does model reduction impact network topology and the subsequent manufacturability evaluation?’. The following hypotheses were proposed to answer the research questions, (i) ‘manufacturability increases as the mesoscale network topology approximates that of a solid sphere’, and (ii) ‘the reduced-order network representation reveals underlying geometric complexity in the crumpled structure’. The hypotheses are addressed in a case study demonstrating the proposed framework for network approximation and model reduction. Model reduction is achieved through analysis of the eigenvalue spectra and reduction of a network approximation of the CAD geometry, eliminating insignificant eigenvalues in the model to reduce spatial redundancies. The case study compares the mesostructure geometry of five crumpled structures with varying compaction ratios ranging from 20% to 100% compaction. The crumpled geometries are also analyzed in comparison to an ideal, solid mesostructure for AM. Topological network properties are measured and evaluated in terms of manufacturability. Topological network properties and manufacturability evaluation results from the case study are summarized in Table 2.

Table 2 Summary of manufacturability evaluation metrics and observed outcomes of the case study.

Index	Topological Network Property	Relationship to the Crumpled Geometry	Manufacturability Evaluation	Observations from the Case Study: High-Order Model	Observations from the Case Study: Reduced-Order Model
1	Geometric area ratio of the giant component size across the structure, comparing crumpled geometries to an 'ideal' mesostructure, a solid sphere (Fig. 5, 6).	An indication of layer-by-layer material deposition, uniform distribution of the giant component across the structure indicates fewer voids and internal overhangs.	More manufacturable as the area ratio approaches 1 (fully dense mesostructure).	Area ratio is monotonically increasing with compaction. Results indicate that the crumpled geometry at 100% compaction most closely approximates the ideal mesostructure.	Area ratio is monotonically increasing with compaction ratio. Dimensionality reduction reveals a prediction of lower manufacturability at $\leq 80\%$ compaction.
2	Average shortest path length (ASPL), the average number of edges along the shortest path between each node pair (Fig. 7).	Shorter ASPL indicates a more homogeneous distribution of ridge lengths in the crumpled sheet and a more uniform distribution of material across the mesostructure. More uniform material distribution may in turn minimize the risk of manufacturing defect propagation across the structure.	Shorter ASPL is associated with more homogeneous, and subsequently more manufacturable, mesostructure geometry.	ASPL monotonically decreasing with compaction ratio, indicate that the crumpled geometry at 100% compaction has the most homogeneous mesostructure, and is therefore the most manufacturable.	ASPL decreases between 20% to 40% compaction, increases at 60% compaction, and decreases again at 80% and 100% compaction. Shortest ASPL is achieved at 100% compaction. Results indicate an inhomogeneous transition point in the distribution of ridge lengths, between 40% and 80% compaction.
3	Node degree distribution, the number of edges per node (Fig. 8, 9).	High node degrees occur along narrow ridges and tightly folded layers in the crumpled sheet. Normal distribution of node degrees is expected to produce a more uniform mesostructure.	More manufacturable as the frequency of node degrees across the network approach a normal distribution.	None of the geometries approach a normal distribution prior to dimensionality reduction, due to spatial redundancy in the high-order representation.	The crumpled geometry at 80% compaction (followed by 100% and 60% compaction) most closely approximates the normal node degree distribution of the solid sphere.

The results in Table 2 are not entirely consistent in predicting a compaction ratio that will reduce the likelihood of structural defects during AM. Even so, the crumpled structure at 100%

compaction performs well with respect to each metric. This performance is attributed to the more uniform distribution of material at high compaction ratios, closely approximating the homogeneous mesostructure of a solid sphere. Manufacturability metric 1 and 3 in Table 2 accord with the first hypothesis, in which the crumpled mesostructure that most closely approximates the solid sphere (in this case, 100% compaction) is predicted to be the most manufacturable by additive processes. Metric 2 diverges from the first hypothesis because shorter ASPL is attributed to increased manufacturability, but the solid sphere exhibits longer ASPL than the crumpled geometries (Figure 7). This discrepancy is attributed to the lack of an analogous ridge network in the solid sphere to compare to the crumpled geometries. Subsequent research may identify an ideal geometry that is suitable for all three metrics listed in Table 2, but at present it is sufficient to minimize ASPL of the crumpled geometry, rather than comparing it to a solid sphere. The results in Table 2 suggest that multiple topological properties should be measured to gain a more comprehensive understanding of the manufacturability of a crumple-formed structure, because each property provides information on a different aspect of the mesoscale geometry.

The second hypothesis states that dimensionality reduction reveals underlying complexity in the crumpled geometry. Comparison of the topological network properties before and after dimensionality reduction summarized in Table 2 demonstrate that the low-dimensional approximation achieved through eigenvalue decomposition provides a more coherent representation of mesoscale complexity by eliminating redundant spatial information in the network representation. Subsequent research will include a more exhaustive investigation of the relationship between the degree of eigenvalue reduction and the resulting network approximation, balancing spatial redundancy, computational expense, and information loss. In following research, complex network theory will also be applied to study the relationship between design inputs and the resulting macroscale properties of crumpled geometries, allowing designers to tailor crumpled geometries to meet specific design requirements. Furthermore, experimental model validation will be performed to analyze how the predicted manufacturability relates to physical defects in AM crumpled structures. X-ray computed tomography and image analysis techniques will be applied to characterize structural deviation between designed and manufactured mesostructure, and to quantify the robust relationship between mesoscale defects and macroscale properties of additively manufactured crumpled geometries. Finally, further research will assess the generality of the proposed manufacturability analysis approach when applied to other geometries with multiscale complexity.

References

- [1] A. Bloesch-Paidosh and K. Shea, “Enhancing Creative Redesign Through Multimodal Design Heuristics for Additive Manufacturing,” *J. Mech. Des.*, vol. 143, no. October, 2021, doi: 10.1115/1.4050656.
- [2] B. Mota and S. Herculano-Houzel, “Cortical folding scales universally with surface area and thickness, not number of neurons,” *Science (80-.)*, vol. 349, no. 6243, pp. 74–77, Jul. 2015, doi: 10.1126/science.aaa9101.
- [3] J. R. Underhill and S. Paterson, “Genesis of tectonic inversion structures: Seismic evidence for the development of key structures along the Purbeck-Isle of Wight Disturbance,” *J. Geol. Soc. London.*, vol. 155, no. 6, pp. 975–992, Nov. 1998, doi: 10.1144/gsjgs.155.6.0975.

- [4] E. H. Jo, H. D. Jang, H. Chang, S. K. Kim, J. H. Choi, and C. M. Lee, “3 D Network-Structured Crumpled Graphene/Carbon Nanotube/Polyaniline Composites for Supercapacitors,” *ChemSusChem*, vol. 10, no. 10, pp. 2210–2217, May 2017, doi: 10.1002/cssc.201700212.
- [5] Sudirja, A. Hapid, S. Kaleg, A. C. Budiman, and Amin, “The Crumple Zone Quality Enhancement of Electric Cars Bumper Fascia using a Carbon Fiber Reinforced Vinyl Ester - Microsphere Composites,” in *Proceeding - 2019 International Conference on Sustainable Energy Engineering and Application: Innovative Technology Toward Energy Resilience, ICSEEA 2019*, Oct. 2019, pp. 108–121, doi: 10.1109/ICSEEA47812.2019.8938633.
- [6] M. J. Mirzaali, M. Habibi, S. Janbaz, L. Vergani, and A. A. Zadpoor, “Crumpling-based soft metamaterials: the effects of sheet pore size and porosity,” *Sci. Rep.*, vol. 7, no. 1, p. 13028, Dec. 2017, doi: 10.1038/s41598-017-12821-6.
- [7] M. C. Fokker, S. Janbaz, and A. A. Zadpoor, “Crumpling of thin sheets as a basis for creating mechanical metamaterials,” *RSC Adv.*, vol. 9, no. 9, pp. 5174–5188, 2019, doi: 10.1039/C8RA07565D.
- [8] M. Habibi, M. Adda-Bedia, and D. Bonn, “Effect of the material properties on the crumpling of a thin sheet,” *Soft Matter*, vol. 13, no. 22, pp. 4029–4034, Jun. 2017, doi: 10.1039/C6SM02817A.
- [9] A. B. Croll, T. Twohig, and T. Elder, “The compressive strength of crumpled matter,” *Nat. Commun.*, vol. 10, no. 1, p. 1502, 2019, doi: 10.1038/s41467-019-09546-7.
- [10] G. Allaire, C. Dapogny, R. Estevez, A. Faure, and G. Michailidis, “Structural optimization under overhang constraints imposed by additive manufacturing technologies,” *J. Comput. Phys.*, vol. 351, pp. 295–328, 2017, doi: 10.1016/j.jcp.2017.09.041.
- [11] A. Blösch-Paidosh and K. Shea, “Design heuristics for additive manufacturing,” *Proc. Int. Conf. Eng. Des. ICED*, vol. 5, no. DS87-5, pp. 91–100, 2017.
- [12] K. Matouš, M. G. D. Geers, V. G. Kouznetsova, and A. Gillman, “A review of predictive nonlinear theories for multiscale modeling of heterogeneous materials,” *J. Comput. Phys.*, vol. 330, pp. 192–220, 2017, doi: 10.1016/j.jcp.2016.10.070.
- [13] S. K. Gupta, W. C. Regli, D. Das, and D. S. Nau, “Automated Manufacturability Analysis : A Survey,” *Res. Eng. Des.*, vol. 9, pp. 168–190, 1997.
- [14] Z. Li, B. Wen, and N. Zabarar, “Computing mechanical response variability of polycrystalline microstructures through dimensionality reduction techniques,” *Comput. Mater. Sci.*, vol. 49, no. 3, pp. 568–581, Sep. 2010, doi: 10.1016/j.commatsci.2010.05.051.
- [15] E. Coatanéa *et al.*, “Systematic manufacturability evaluation using dimensionless metrics and singular value decomposition: a case study for additive manufacturing,” *Int. J. Adv. Manuf. Technol.*, 2020, doi: 10.1007/s00170-020-06158-0.
- [16] A. Dong and S. Sarkar, “Forecasting technological progress potential based on the complexity of product knowledge,” *Technol. Forecast. Soc. Change*, vol. 90, no. PB, pp. 599–610, 2015, doi: 10.1016/j.techfore.2014.02.009.
- [17] S. Sarkar, A. Dong, J. A. Henderson, and P. A. Robinson, “Spectral characterization of hierarchical modularity in product architectures,” *J. Mech. Des. Trans. ASME*, vol. 136, no. 1, 2014, doi: 10.1115/1.4025490.
- [18] T. Tallinen, J. A. Ström, and J. Timonen, “The effect of plasticity in crumpling of thin sheets,” *Nat. Mater.*, vol. 8, no. 1, pp. 25–29, 2009, doi: 10.1038/nmat2343.

- [19] G. A. Vliegenthart and G. Gompper, “Forced crumpling of self-avoiding elastic sheets,” *Nat. Mater.*, vol. 5, no. 3, pp. 216–221, Mar. 2006, doi: 10.1038/nmat1581.
- [20] A. A. Hagberg, D. A. Schult, and P. J. Swart, “Exploring network structure, dynamics, and function using NetworkX,” *7th Python Sci. Conf. (SciPy 2008)*, no. SciPy, pp. 11–15, 2008.
- [21] A. Dong and S. Sarkar, “Design Computing and Cognition ’12,” *Des. Comput. Cogn. ’12*, pp. 415–432, 2014, doi: 10.1007/978-94-017-9112-0.
- [22] D. Braha and Y. Bar-Yam, “The statistical mechanics of complex product development: Empirical and analytical results,” *Manage. Sci.*, vol. 53, no. 7, pp. 1127–1145, Jul. 2007, doi: 10.1287/mnsc.1060.0617.